

# 공초점 현미경을 이용한 마이크로믹서 내부의 3 차원 이미지화

김현동\* · 김경천†

## 3-D Imaging in a Chaotic Micromixer Using Confocal Laser Scanning Microscopy (CLSM)

Hyundong Kim and Kyung Chun Kim

### Abstract

3-D visualization using confocal laser scanning microscopy (CLSM) in a chaotic micromixer was performed as a reproduction experiment and the feasibility of 3-D imaging technique in the microscale was confirmed. For diagonal micromixer (DM) and two types of staggered herringbone micromixers (SHM) designed by Whitesides et al., to verify the evolution of mixing, cross sectional images are reconstructed at the end of every cycle. In a DM, clockwise rotational flow motion generated by diagonal ridges placed on the floor of micromixer is observed and this motion makes the fluid commingle. On the contrary, there are two rotational flow structures in the SHM and the centers of rotation exchange their position each other every half cycle because of the V shape of ridges varying their orientation every half cycle. Local rotational flow and local extensional flow generated by the complicate ridge pattern make the flow be chaotic and accelerate the mixing of fluid. The dominant parameter that influences on the mixing characteristic of SHM is not the length of micromixer but the number of ridges under the same flow configurations.

**Key Words :** Confocal Laser Scanning Microscopy(공초점 현미경), Micromixer(마이크로믹서), Optical Slicing(광학적 분할), Three Dimensional Imaging(3 차원 영상)

### 1. 서 론

3-dimensional imaging is not easily achievable in micro-scale. Some techniques based on interferometry, projected fringe can measure surface topography but it is impossible to image inside of specimen. Computer deconvolution

technique to enhance images of through-focal series using epi-fluorescence microscopy has inherent limitation of image quality. Another method for 3-D imaging, physical slicing of specimen, also causes new problems such as deformation of specimen, align in 3-D reconstruction process and fitness for living cell.

However, the concept of confocal microscopy pioneered to image the neural networks in preparation of brain tissue by Marvin Minsky in 1955 has been evolved as a promising technique for 3-D imaging in micro-scale. The fundamental concepts of confocal,

---

† 부산대학교 기계공학부

E-mail : kckim@pusan.ac.kr

\* 부산대학교 일반대학원 기계공학과

point illumination and spatial filtering of light emanating from focal point by pinhole aperture at confocal point, improve lateral and axial resolutions of microscopy drastically. Moreover, a capability of depth wise optical sectioning without physical slicing of specimen and 3-D imaging provide explosive applications to biology, materials, medical research and microfluidics.

Especially for the microfluidic applications, Knight et al. (1998) adopted confocal laser scanning microscopy to describe mixing by means of hydrodynamic focusing in a silicon chip and demonstrated 3-D structure of fluid jet. Similarly, Whitesides et al. (2000) quantified diffusion across the interface between two aqueous solutions in microchannel and verified the performance of chaotic micromixers by visualizing panoramic cross section images (2002). Park et al. (2004) first developed optically sliced microscopic particle image velocimetry (micro-PIV) using CLSM, and applied the CLSM micro-PIV and the conventional epi-fluorescence micro-PIV to Poiseuille flows in a 100  $\mu$  m diameter capillary. A fully developed horizontal laminar flow was mapped at several depthwise planes and results were compared with the predictions based on the Poiseuille flow fields. They showed that CLSM micro-PIV improved image contrasts, definitions, and accuracy of velocity field measurement. Park et al. (2002) also measured velocity field around a moving bubble in a 100  $\mu$  m square channel by using CLSM. They achieved optically sectioned flow velocity mapping for the region ahead of the moving air bubble.

Besides these results, optical slicing capability of confocal microscopy has great potential for measurement of microfluidic characteristics such as laser induced fluorescence (LIF), temperature measurement. Therefore, it is important to understand the principle of confocal microscopy and master the 3-D imaging technique for the materialization of this potential. In this work, to practice the 3-D imaging technique using CLSM and verify its feasibility, experiments of cross sectional visualization in a chaotic micromixers designed by Whitesides et al. (2002) have been conducted.

## 2. Optical resolutions and image slicing

In microscopic system, optical resolutions are restricted by the numerical aperture of optical components and by the wavelength of light, both excitation and emission. The concept of resolution is defined as the minimum separation between two points that results in a certain level of contrast between them and point spread function (PSF) of optical system is used to specify the resolution.

However, optical resolutions of confocal microscopy are affected by its unique configuration. There are two PSF, PSF of the illuminating light source and PSF of the emitting light, and the image resolution is determined by the product of between two PSF. Also pinhole diameter of confocal microscopy is an important parameter for theoretical analysis of resolutions and optical slicing. If modified pinhole diameter, PD, is larger than airy unit, AU, i.e.,  $PD > AU$ , a geometric-optical analysis can be used. On the other hand, if PD is smaller than 0.25AU, a wave-optical analysis is applied. (Wilhelm et al. 2003) Where PD is defined as (pinhole diameter in  $\mu$  m) / magnification, and AU is defined as  $1.22 \lambda_{ex} / NA$ . Where NA is numerical aperture of objective and  $\lambda_{ex}$  is fluorescent excitation wavelength. By means of this classification, the optical resolutions and optical slice thickness of CLSM are defined differently and these are defined in table 1. The lateral resolution uses a criterion based on full-width at half-maximum (FWHM) of two neighboring PSF images at the confocal plane and axial resolution is based on the FWHM of PSF presented along the optical axis.

In the geometric-optical confocal microscope with sufficiently small PD, the lateral and axial resolution are specified by functions of mean wavelength  $\bar{\lambda}$ , of excitation wavelength,  $\lambda_{ex}$ , and emission wavelength,  $\lambda_{em}$ , because FWHM of illumination PSF and emission PSF are comparable in their magnitudes. Where  $\bar{\lambda}$  is given by

$$\bar{\lambda} = \sqrt{2} \frac{\lambda_{ex} \lambda_{em}}{\sqrt{\lambda_{ex}^2 + \lambda_{em}^2}} \quad (1)$$

On the other hand, for the geometric-optical confocal microscope with larger PD, the FWHM

Table 1. Lateral and axial resolution and optical slice thickness of confocal microscopy (Wilhelm et al. 2003; Park et al. 2004)

		Geometric-optical confocal microscope	Wave-optical confocal microscope
Lateral resolution		$\frac{0.51\lambda_{ex}}{NA}$	$\frac{0.37\bar{\lambda}}{NA}$
Axial resolution	NA ≥ 0.5	$\frac{0.88\lambda_{ex}}{n - \sqrt{n^2 - NA^2}}$	$\frac{0.64\bar{\lambda}}{n - \sqrt{n^2 - NA^2}}$
	NA < 0.5	$\frac{1.67n \cdot \lambda_{ex}}{NA^2}$	$\frac{1.28n \cdot \bar{\lambda}}{NA^2}$
Optical slice thickness		$\sqrt{\left(\frac{0.88\lambda_{ex}}{n - \sqrt{n^2 - NA^2}}\right)^2 + \left(\frac{\sqrt{2n} \cdot PD}{NA}\right)^2}$	$\frac{0.64\bar{\lambda}}{n - \sqrt{n^2 - NA^2}}$

Table 2. Optical parameters and slice thickness depending on the magnification for n = 1.47 (glycerin and water mixture),  $\lambda_{ex} = 543 \text{ nm}$ ,  $\lambda_{em} = 575 \text{ nm}$ ,  $\bar{\lambda} = 558 \text{ nm}$ .

	Magnification	NA	Working Distance (μm)	PD (μm)	Airy unit (AU)	Optical slice Thickness (μm)
HC PL APO CS	20 X	0.7	590	8.9	0.946	26.58
HGX PL APO (Oil)	40 X	1.25	100	4.45	0.53	7.44
HGX APO (Water)	63 X	0.9	2200	2.825	0.736	6.7

of the emission PSF is larger than that of illumination PSF and the functions of only  $\lambda_{ex}$  specify the optical resolutions (Park et al. 2004). Likewise the optical slicing capability, which plays crucial role in 3-D imaging, can be explained from the PSF of confocal microscopy. The illumination PSF and emission PSF, they two are independent events mathematically, and the PSF of confocal microscopy is represented by the product of two PSF. At the confocal plane, magnitude of emission PSF has maximum value, but the farther a point is off the focal plane the more drastic signal decrease. Finally, it gets so weak at some distance that it is well below the detecting threshold of the system then is no longer detectable. This mechanism allows optical slicing of specimen and provides information for 3-D image reconstruction. The optical slice thickness of confocal microscopy was developed theoretically with experimental corrections by multiple contributors and tabulated in Table 1.

Table 2. presents optical parameters and optical slice thickness depending on magnification for this study. Optical slice thickness is calculated for 178 μm of pinhole diameter and 1.47 of refractive index in a

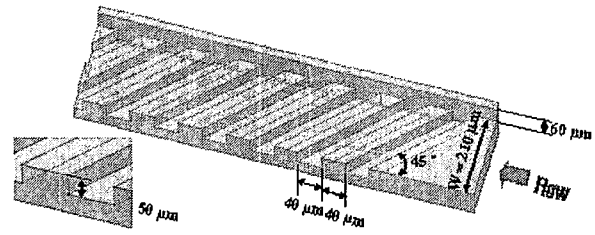


Fig. 1 Channel geometry used for 3-D visualization experiment. Main channel cross section has 210 μm wide and 60 μm height. Width and pitch is 40 μm.

geometric-optical confocal microscope criterion ( $PD > AU$ ). 543 nm of excitation light and 575 nm of emission light are used for imaging and corresponding mean wavelength is 558 nm. The optical slice thickness is estimated to be less than 7 μm for the 63X-0.7NA objective and less than 27 μm for the 20X-0.7NA objective.

### 3. Experiments

#### 3.1 Chaotic micromixer

Originally, the chaotic micromixer used in this study is designed by Whitesides et al. in 2002 and fabricated by Memstec in Korea to verify 3-D velocity field measurement technique in a microchannel. One type of diagonal mixer (DM) and two types of staggered herringbone mixer (SHM) are used for present work.

Fig. 1 shows the shape of DM and its dimensions. The main channel has rectangular cross-section of 210μm wide and 60μm high, and diagonal ridges with 45 degree to initial flow direction are placed to make spanwise velocity element on the floor of channel. The width and pitch of ridges are 40μm and its height is 50μm. As shown in Fig. 5, SHM has V shape of ridges to provide an anisotropic resistance to viscous flow and 12 ridges make 1 cycle. The main channel of SHM has same dimension with the DM and width of ridge is also 40μm, but the pitch of third model ( Fig. 5b ) is 80μm.

This type of micromixers can be fabricated with two-step of photolithography using SU-8. The first layer of photolithography defined channel structure and second layer defined pattern of ridges. After alignment of these two layers using mask aligner, fabrication was completed with PDMS molding process and then

PDMS mold is bonded to slide glass in a plasma asher.

### 3.2 Experimental setup

The experimental setup (Fig.2) consist of a confocal laser scanning microscopy (TCS SP2, Leica), a 543nm Ar / Kr laser, a micro syringe pump (55-2111, Harvard Apparatus), an imaging software (Leica confocal software, Leica).

As a working fluid glycerin (Fisher scientific) and water mixture (80% glycerin and 20% water, mass fraction) were used because of its low diffusivity. If the diffusivity of working fluid is high, it is difficult to observe clear borderline and development of mixing process. Density of working fluid is 1260kg/m<sup>3</sup> and its dynamic viscosity is 0.06 kg/m• s at 20 °C, and refractive index was 1.47.

For the fluorescence imaging, one syringe is filled with working fluid labeled with rhodamine B ( $\lambda_{ex} = 545\text{nm}$  and  $\lambda_{em} = 575\text{nm}$ , and 1 mM concentration, Sigma-Aldrich) and another one is field with unlabeled mixture. Then two syringes pumped by a micro-pump generate constant flow rate 4.5 $\mu$  l/min and initial fluid velocity calculated based on the flow rate is 6mm/s. The corresponding Reynolds number is 0.0115.

For each case, to clarify the evolution of mixing, cross sectional image is reconstructed from the 130 optically sliced images with the 0.5  $\mu$  m step size at the end of each cycle. This procedure is repeated from first cycle to fifth cycle. These experimental conditions were applied for three different types of micromixers identically.

### 3.3 Decision of interface between microchannel and cover glass

For 3-D reconstruction of optical sliced images, it is essential to define the interface between cover glass and microchannel because the confocal pinhole can not remove the ray emitted from out-of-focal point perfectly. To obtain information about the interface, experiment using T-shape of glass channel was conducted and Fig. 3 presents the optically sliced fluorescent images in a microchannel

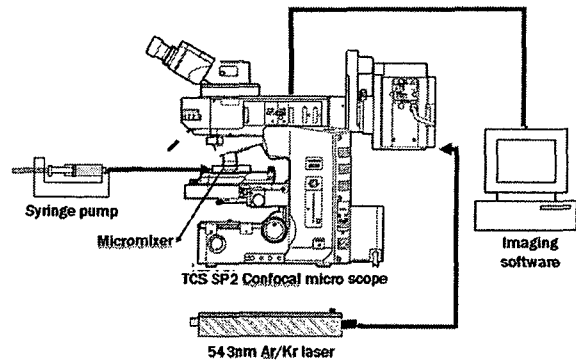


Fig. 2 Experimental setup of 3-D visualization in a chaotic micromixer

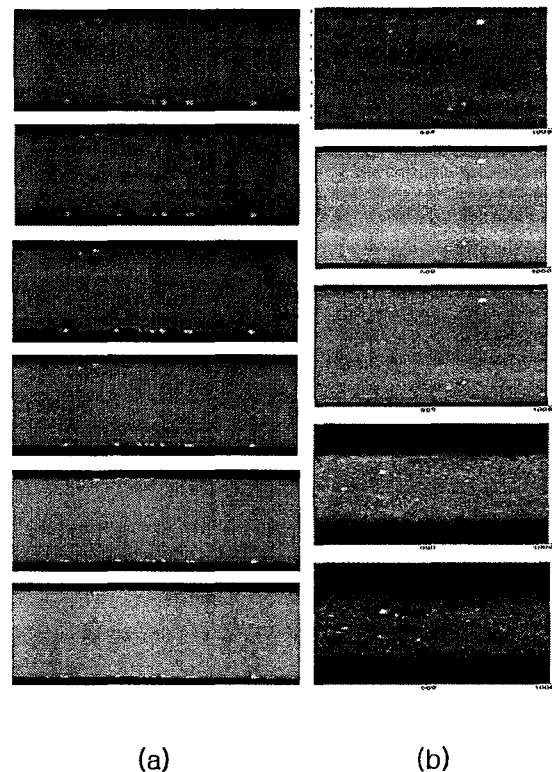


Fig. 3 Confocal fluorescence images of glass microchannel filled with fluorescence dye (rhodamine B) solution to define interface between microchannel and cover glass. (a) Images using 20X-0.7NA dry objective and 2  $\mu$  m step size (b) Images using 63X-0.9NA water immersion objective and 2  $\mu$  m step size

The glass channel is fabricated by dry etching technique in Dong-a university. A cross section of microchannel has 110  $\mu$  m of width at the top surface, 40  $\mu$  m of width at the bottom surface, 40  $\mu$  m of height and 40  $\mu$  m of round

at the wall.

When the 20X-0.7NA dry objective was used for imaging (Fig. 3a), it is very difficult to decide the edge or surface of microchannel due to its thick optical slice thickness ( $27 \mu\text{m}$ ). However, for the case of 63X-0.9NA water immersion objective (Fig. 3b, optical slice thickness =  $6.7 \mu\text{m}$ ), edge line of microchannel is relatively clear and image of bottom surface is distinguished from other images. From these images, the interface and bottom surface can be presumed and optical sectioning range is estimated.

### 3. Results and discussion

The frames in Fig. 4 are cross sectional images of DM reconstructed from optically sliced images. Actually there is not a concept of cycle in the DM, but for the convenience of comparison with the SHM, 12 ridges is defined as one cycle because 1 cycle of SHM also consist of 12 ridges. This figure presents the development of mixing from inlet to after 5th cycle. Due to transverse flows generated by diagonal ridges placed on the bottom of micromixer, clockwise rotational flow motion is occurred over the cross section. This rotational flow motion causes the stretching and folding of fluid which is the basic mechanism of chaotic mixing and then the fluid injected to different inlet is commingled despite of its low diffusivity.

Fig. 5 shows the series of cross-sectional fluorescence images in the SHM. Fig. 8a represents reproduced results under the same experimental conditions with the Whitesides et al. Unlike the case of DM, SHM has V shape of ridges varying their orientation every half cycle. Therefore there exist two rotational flow structure in the SHM and the centers of rotation exchange their position each other every half cycle. Local rotational flow and local extensional flow generated by the complicate ridge pattern make the flow more chaotic and accelerate the mixing of fluid. These effects can be confirmed by comparing the fluorescence images of DM and SHM qualitatively.

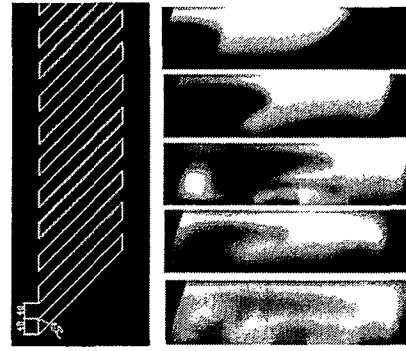


Fig. 4 A series of cross-sectional fluorescence images in a diagonal micromixer

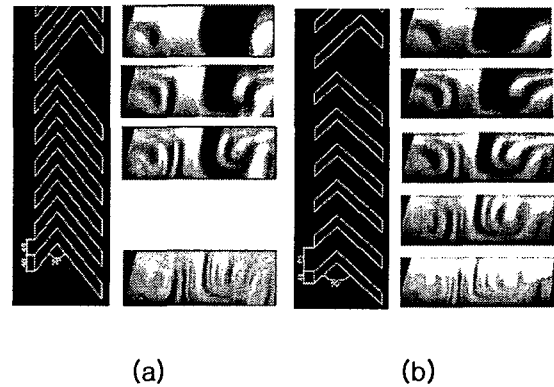


Fig. 5 Series of cross-sectional fluorescence images after first five cycles in SHM (a) results of SHM which has same dimension with Whitesides et al. case (b) results of SHM which has  $80\mu\text{m}$  pitch

On the other hand, as shown in Fig. 5b, when the pitch between ridges in SHM is increased two times, there is not special change in flow motion. This means the dominant parameter that influences on the mixing characteristic of SHM is not the length of micromixer but the number of ridge.

### 4. 결 론

To practice the 3-D imaging technique using CLSM and identify its feasibility, experiments of visualization in a chaotic micromixers designed by Whitesides et al. (2002) was performed, and cross sectional images were reconstructed from optically sliced images.

In a DM, Clockwise rotational flow motion

generated by diagonal groove placed on the bottom of micromixer is observed and this motion allows fluid to be commingled. For the case of SHM, it is confirmed that the reproduced experimental results agree with the results of previous study. Local rotational flow and local extensional flow generated by V shape ridges make the flow more chaotic and accelerate the mixing of fluid. Furthermore, the dominant parameter that influences on the mixing characteristic of SHM is not the length of micromixer but the number of ridge.

### 참 고 문 헌

- 1) Minsky M, 1998, "Memoir on inventing the confocal scanning microscope", *Scanning* 10:128-138.
- 2) James B. Knight, Ashvin Vishwanath, James P. Brody, and Robert H. Austin, 1998, "Hydrodynamic Focusing on a Silicon Chip: Mixing Nanoliters in Microseconds. Physical", *Review Letters* 80: 3863-3866.
- 3) Rustem F. Ismagilov, Abraham D. Stroock, Paul J. A. Kenis, and George Whitesides, 2000, "Experimental and theoretical scaling laws for transverse diffusive broadening in two-phase laminar flows in microchannels.", *Applied Physics Letter* 76: 2376-2378.
- 4) Abraham D. Stroock, Stephan K. W. Dertinger, Armand Ajdari, Igor Mezic, Howard A. Stone, George M. Whitesides, 2002, "Chaotic mixer for microchannels", *Science* 295: 647-651
- 5) Jae S. Park, Chang K. Choi, Kenneth D. Kihm, 2004, "Optically sliced micro-PIV using confocal laser scanning microscopy (CLSM)", *Experiment in Fluids* 37: 105-119.
- 6) Jae S. Park, Kenneth D. Kihm, 2006, "Use of confocal laser scanning microscopy (CLSM) for depthwise resolved microscale particle image velocimetry ( $\mu$ -PIV)", *Optics and Lasers in Engineering* 44: 208-223.
- 7) Webb H. Rober, 1996, "Confocal optical microscopy.", *Reports on Progress in Physics* 59: 427-471.
- 8) Hans J. Tiziani and Hans-Martin Uhde, 1994, "Three-dimensional analysis by a microlens-array confocal arrangement", *Applied optics* 33: 567-572.